

# Impulse noise detection technique based on fuzzy set

V.P. Ananthi<sup>1,2</sup>, P. Balasubramaniam<sup>1</sup>✉, P. Raveendran<sup>3</sup>

<sup>1</sup>Department of Mathematics, Gandhigram Rural Institute – Deemed University, Gandhigram – 624302, Tamil Nadu, India

<sup>2</sup>Department of Mathematics, Gobi Arts and Science College, Gobichettipalayam – 638453, Tamil Nadu, India

<sup>3</sup>Department of Electrical Engineering, University of Malaya, Kuala Lumpur, 50603, Malaysia

✉ E-mail: balugru@gmail.com

ISSN 1751-9675

Received on 19th September 2016

Revised 1st July 2017

Accepted on 28th July 2017

E-First on 28th September 2017

doi: 10.1049/iet-spr.2016.0538

www.ietdl.org

**Abstract:** In this study, a new fuzzy-based technique is introduced for denoising images corrupted by impulse noise. The proposed method is based on the intuitionistic fuzzy set (IFS), in which the degree of hesitation plays an important role. The degree of hesitation of the pixels is obtained from the values of memberships of the object and the background of the image. After minimising the obtained hesitation function, the IFS is constructed and the noisy pixels are detected outside the neighbourhood of mean intensity of the object and the background of an image. Denoised images are relatively analysed with five other methods: modified decision-based unsymmetric trimmed median filter, noise adaptive fuzzy switched median filter, adaptive fuzzy switching weighted average filter, adaptive weighted mean filter, iterative alpha trimmed mean filter. Performances of the proposed method along with these five state-of-the-art methods are evaluated using a peak signal-to-noise ratio and error rate along with the time for computation. Experimentally, derived denoising method showed an improved performance than five other existing techniques in filtering noise in images due to the reduction of uncertainty while choosing the noisy pixels.

## 1 Introduction

Existence of noise in images is a primary issue in image processing. Another important problem is, its removal using a technique with non-degrading property. Typically, digital images are corrupted by impulse noise during image acquisition due to imperfection in sensors or during transmission through communication channels [1, 2], which cause inverse impact in subsequent steps of processing like partitioning and object detection in computer vision. Random-valued noise [3] and salt-and-pepper noise (SPN) [4] are the impulse type noises that affect images. Unlike other types of noises, impulse noise affects only some portions of the image.

Main aim of filtering noise in images is to reduce noise without degradation of image features. This problem could be rectified by using the appropriate filter. Non-linear filters are more effective in reducing noise without degradation in image features than linear filters [5]. The median filter is a rank order filtering scheme which performs better than linear filters but the median filter smoothed edges and blurs the fine details in images [6]. In order to overcome this issue, several state-of-the-art filtering techniques have been emerged such as adaptive weighted mean filter (AWMF) [4], optimal weighted median filter [7], adaptive median filter [8], tristate median filter [9], switched median filter [10], adaptive centre weighted median filter [11], adaptive fuzzy switching weighted average filter (AFSWAF) [12], progressive switching median filter [13], noise adaptive fuzzy switched median filter (NAFSMF) [14, 15], modified decision-based unsymmetric trimmed median filter (MDBUTMF) [16], non-local mean filters [17, 18] and iterative alpha trimmed mean filter (IATMF) [5]. Among them, we focus on the five filters namely, MDBUTMF, NAFSMF, AFSWAF, AWMF and IATMF for their efficiency.

MDBUTMF in [16], has explored noisy candidate in images affected with SPN via the extreme intensity values, 0 and 255. Then, the mean variants of their respective  $3 \times 3$  filter windows have been adaptively identified as denoised brightness level. Instead of a fixed filtering window size, NAFSM has utilised the histogram of the corrupted image to identify noisy pixels and later fuzzy reasoning has been utilised to restore the impulse that was

detected. However, the noise detection stage is very simple and there is a possibility of misclassification of uncorrupted pixels when impulse is more. AFSWAF method has incorporated fuzzy functions ‘small’ in switching filter for detecting uncorrupted pixels. A modified version of Gaussian function has been utilised to determine the similarity among the detected uncorrupted pixels for good restoration. The corrupted pixels were restored by weighted mean of the filtering window.

SPN has been reduced using AWMF by enlarging the window size continuously until the maximum and minimum values of two successive windows, respectively, have equal values [4]. Then the considered pixel of extreme values has been replaced by the weighted mean of the current window, other pixels left unaltered. Noisy and good pixels have been identified using IATMF by checking the intensity value of the considered pixel is an extreme value. Initial filtering window size has been chosen as  $3 \times 3$  and it has been increased till the stopping criterion based on good pixel set has reached. Then, the identified noisy pixel in that window has been replaced by mean value of their neighbour. Here, the denoising techniques have detected the noisy pixel by relating them directly or indirectly to the intensity value either 0 or 255. In case an image contains 255 as its original brightness level, then the above techniques may consider those pixels for denoising. The above discussion motivates us to develop an algorithm that does not rely on extreme intensity values during noise detection.

Mostly differential models were used to find edges of an image. But fractional ordered differential models have been developed in last decade to solve image distortion, which provides an enhanced denoising mask for noise removal [19]. Further in the literature, some techniques have been available for the restoration of noise in digital images based on adaptive filtering [20–23], on clustering algorithm [24] and on principal component analysis [25].

Generally pixels with impulse noise have extreme intensity level than that of the surrounding pixels. Visually one can see the effect of impulse noise after an average filter is applied by convolving the noise impaired pixel with a small window [5]. Extending the same concept, a new method is proposed to reduce SPN using square filtering window. In television pictures direct replacement of pixels by average filter might possess some

disadvantages, which may reduce the resolution of the pictures. In order to avoid this effect, a fuzzy-based noise removal technique is introduced.

Fuzzy sets (FSs) are initially introduced to deal vagueness [26]. Usually in images, vagueness arises in assigning brightness value to a pixel. But in the case of noisy images, vagueness arises in the selection of non-noisy pixels from a group of noisy ones using their vague brightness level and such vagueness is addressed in terms of hesitation degree. In this paper, hesitation of an expert is considered as assigning the membership value to a noisy pixel. A method is introduced to reduce the hesitation there by producing an appropriate FS for noise removal. Situations like reducing hesitation in the selection of noisy candidate can be effectively handled by using intuitionistic fuzzy sets (IFSs), which was introduced by Atanassov [27] in 1986. Hesitation degree in the proposed method is generated using entropy, which reflects the visual effects of an image. The proposed detection scheme consists of two phases of detection. In the first phase, a fuzzy image is convolved with kernels in all directions to find out the pixels in image with impulse. The second detection phase detects noisy pixels by a IFS with minimum entropy. Finally, the results from these two detection units are combined to get a more robust noise detection method for improving global performance. Finally, the noisy candidates are denoised by employing a fuzzy-based denoising filter.

This paper is organised as follows. Section 2 explains some works related to the present study. Section 3 discusses the algorithm of the proposed mechanism of detection and filtering. Simulation results and the values of quantitative measures are analysed in Section 4. Finally, conclusions are drawn in Section 5 with future directions.

## 2 Existing denoising methods and the necessity for introducing the proposed filtering method

Median filtering is a non-linear filtering technique and based on this filter, numerous algorithms have been initiated to reduce noise in images [6]. Some of the available filtering techniques in [4, 5, 12, 15, 16] are utilised for comparing the proposed method of denoising. Each noise removal technique is briefly explained below.

Adaptive filtering process has been combined with switched median denoising technique in [15] and regenerated a new technique called as NAFSMF. NAFSMF searches high and least grey levels in the image for localisation of noisy pixels based on histogram. Initial filtering window size has been fixed as  $3 \times 3$  and searching for one single nearer pixel of the considered noisy pixel, which is related to set of noise free pixels (i.e. other than 0 and 255). If the neighbour of the considered pixel belongs to the noisy free set, then the intensity was replaced with the median value of pixels in that window. If not, the filtering window size has been expanded continuously till the size  $7 \times 7$  for the detection of noise free pixel in that window. In addition, the fuzzy reasoning has been used to deal with the uncertainty present in the local information and helps to produce a correction term while restoring the detected noisy pixels.

One of the difficulties faced by switching method of denoising is to fix a threshold before initiating the noise detection process [16]. MDBUTMF has been implemented to extinguish such trouble during denoising. Only peak values (0 and 255) of the image element were considered for denoising and others kept unchanged, because it has been initiated for SPN. Noisy image elements were altered by a mean value of  $3 \times 3$  neighbour if its  $3 \times 3$  neighbour has only extreme values; rather, it has been altered using median value of its  $3 \times 3$  neighbour. Iteratively, the same procedure is being done till each noisy image element has been processed.

In AWMF [4], noisy candidates have been selected based on the extreme intensity values. Window size in AWMF has been chosen, so that two successive windows should have same extreme values. For instance, initially the minimum and maximum values in a  $3 \times 3$  window around the noisy candidate were found. Then the extreme values in the next window of size  $5 \times 5$  have to be estimated. If the minimum and maximum values were same in both the windows,

and then the window of size  $3 \times 3$  has been considered as an adaptive size for filtering. Else, iteratively size of the window has been increased by 1 till the window of maximum size  $79 \times 79$  in search of attaining the termination condition. Weighted median value of the neighbours related to the considered noisy pixel in the selected window had been estimated and replaced in the place of the intensity value of the noisy candidate.

Initially in IATMF [5], some  $K$  pixels have been selected as non-noisy in a window of size  $3 \times 3$ . Then, a pixel has been chosen from that window for testing whether it is noisy or non-noisy. If the value of the pixel is neither 0 nor 255, then it has been kept unaltered by taking it as noiseless. Otherwise, the degree of membership value of the considered pixel has been computed by using the Gaussian membership function. If the membership value is found to be lesser than a threshold  $h_0$ , then the corresponding pixel had been considered noisy; otherwise, it is considered as non-noisy. Good pixel set  $G$  has been generated by calculating intensity values of the neighbouring pixels in the considered window, in which each element has membership value greater than  $h_0$ . If its count  $|G| < K$ , then one can have some good pixels in the noisy set. For such case,  $h_{\max} = h_0$  has been reduced to  $h_{\min}$  and the steps were repeated till the freezing condition  $|G| \geq |K|$  is met. Suppose if the condition  $|G| < |K|$  is even unchanged, then the window size of order 3 has been increased to the order 5 until the stopping criteria have reached. Once the criterion is satisfied, the considered pixel was chosen to be noisy. A distance weighted function has been utilised to find the weights of the median filter.

AFSWAF [12] technique has relatively the same procedure as in [5] for finding noisy pixels based on the Gaussian membership function and similarity measure in fuzzy domain. Here, the window size had been fixed as  $3 \times 3$  and the size is increased consequently along with the increment of the thresh value. Weighted mean filtering had been applied for replacing the intensity value of the chosen noisy pixels. It has been noticed that this method also detects noisy candidate based on either 0 or 255. Recently, threshold-based selection of corrupted pixels has been investigated for colour images in [28].

Exploring the noisy candidate in the above-mentioned techniques may results in unconventional choice, because the detection of noisy pixels using the greyness 0 and 255 might not belong to the set of noisy pixels. Hence, this leads to filtering error. Visual image feature can be studied using entropy of the considered image. These techniques of filtering have not taken such strategy while filtering. Another difficulty faced by the above algorithms is in the selection of pre-defined threshold. Above discussion propels to introduce a technique, which integrates entropy for selecting noisy candidate using FS and segmenting images by finding a separate thresh value for each images for finding appropriate noisy candidate.

Generally, image is fuzzy due to numerous levels of brightness and such fuzziness is concentrated in the proposed method. But there arises hesitation while assigning the amount of brightness to the pixels of noisy image, such assignment depends wholly on the chosen membership function of FSs and can be reduced by using IFS. Such uncertainty has not been taken into account while filtering images by these existing papers. The above-discussed existing filtering methods also find the noisy candidate by searching intensity values of the image as 0 and 255. Principal objective of the proposed filtering is to eliminate noise by searching the noisy candidate without concerning their extreme values.

## 3 Algorithm of the proposed method

Before going into the description of the proposed algorithm, some preliminary ideas of FS and IFS are demonstrated that are used in the sequel.

### Fuzzy sets

Let  $X$  be a finite set. A FS [26]  $F$  in  $X$  with  $M$  number of elements is defined as

$$F = \{(x, \mu_F(x)) | x \in X\}$$

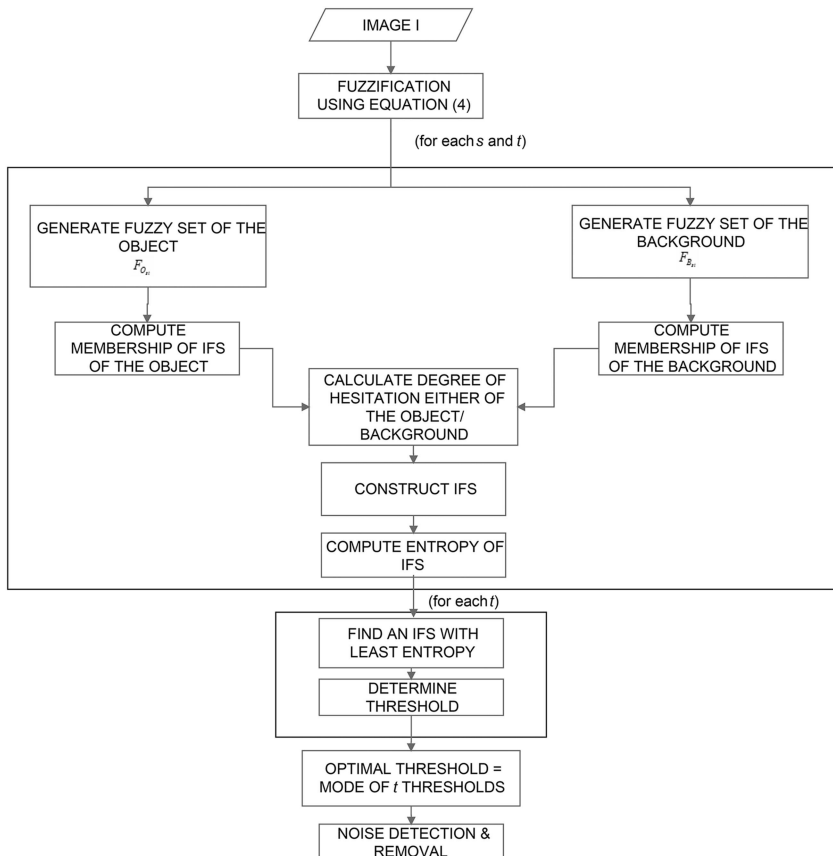


**Fig. 1** Flowchart of the proposed second detection unit

where the function  $\mu_F(x): X \rightarrow [0, 1]$  symbolises the membership degree of  $x$  in  $X$  and its non-membership degree is  $1 - \mu_F(x)$ .

#### Intuitionistic FSs

An IFS [27]  $A$  on  $X$  may be mathematically computed as

$$A = \{(x, \mu_A(x), \nu_A(x)) | x \in X\}$$

where the functions  $\mu_A(x), \nu_A(x): X \rightarrow [0, 1]$  respectively represent the belongingness and non-belongingness of an element  $x$  in  $X$  with an essential condition  $0 \leq \mu_A(x) + \nu_A(x) \leq 1$ . Due to lack of knowledge of an expert in the allotment of appropriate membership function for each image there arises hesitation, which is represented by hesitation degree  $\pi_A(x) = 1 - \mu_A(x) - \nu_A(x)$ . By utilising this degree an IFS  $A$  can be defined as

$$A = \{(x, \mu_A(x), \nu_A(x), \pi_A(x)) | x \in X\}$$

and the condition  $\mu_A(x) + \nu_A(x) + \pi_A(x) = 1$  holds.

The proposed method uses two detection units to find the affected pixels caused by the noise. The first noise detection unit works on fuzzy domain, while the second noise detection unit works on intuitionistic fuzzy domain, where the degree of hesitation plays an important role. In the first noise detection unit, the image is convolved with the directional filters for detecting noisy pixels. While in the proposed second detection unit, several tasks are done to find the best threshold to identify noisy pixels. Flowchart of the proposed second detection unit is shown in Fig. 1.

### 3.1 First noise detection unit

The first step is based on convolution of the corrupted input image with eight one-dimensional kernels of  $2k+1, k \geq 1$  that are sensitive to edges in different directions. The minimum absolute value of these eight convolutions is then compared with a threshold value as a necessary condition for a pixel to be classified as noisy.

Consider an image  $I$  corrupted by noise. Here hesitation arises due to various levels of brightness in the noisy image  $I$ , which leads to uncertainty in the construction of membership values to those pixels in the image  $I$ . In order to reduce this uncertainty, fuzzy image  $F_I$  is generated by normalising brightness levels of the image  $I$  using

$$F_I = \{(I(i, j), \mu_I(I(i, j))) | 0 \leq I(i, j) \leq L - 1\} \quad (1)$$

where  $\mu_I(I(i, j)): I \rightarrow [0, 1]$  denotes the membership degree of  $(i, j)$ th pixel in  $I$ .

Neighbours of the central pixels  $c$  in eight possible directions (North West, North, North East, East, South East, South, South West, West) are shown in Fig. 2a. Fuzzy image  $F_I$  is convolved with a set of convolution kernels of order  $2k+1$  (here  $k=1$ ) as depicted in Fig. 2b.

By taking minimum of all the eight convolutions as

$$N(I(i, j)) = \min \{|\mu_I(I(i, j)) * K_p| : p = 1 \text{ to } 8\}, \quad (2)$$

where  $K_p$  is the  $p$ th kernel and  $*$  denotes convolution operation. The minimum absolute value of these convolutions is then compared with a threshold value,  $t$ , such that if  $N(I(i, j)) > t$ , then the considered pixel is a possible noise candidate. It should be noted that if  $N(I(i, j))$  is small then the current pixel is noise free; if the value of  $N(I(i, j))$  has at least one convolution is small then the considered pixel is an edge and if  $N(I(i, j))$  has larger convolution value then the pixel is an isolated impulse. Pixels that are detected using the first detection unit will be considered as a possible noisy candidate. The possibly noisy set is considered as noisy if they are salt and pepper noise. A threshold value  $t$  obtained by Otsu's method [29] and is utilised for the detection of noisy pixels. The set of possibly noisy pixels  $\alpha$  can be expressed as

$$\alpha(i, j) = \begin{cases} 1, & \text{if } N(I(i, j)) > t/255; \\ 0, & \text{if } N(I(i, j)) \leq t/255. \end{cases} \quad (3)$$

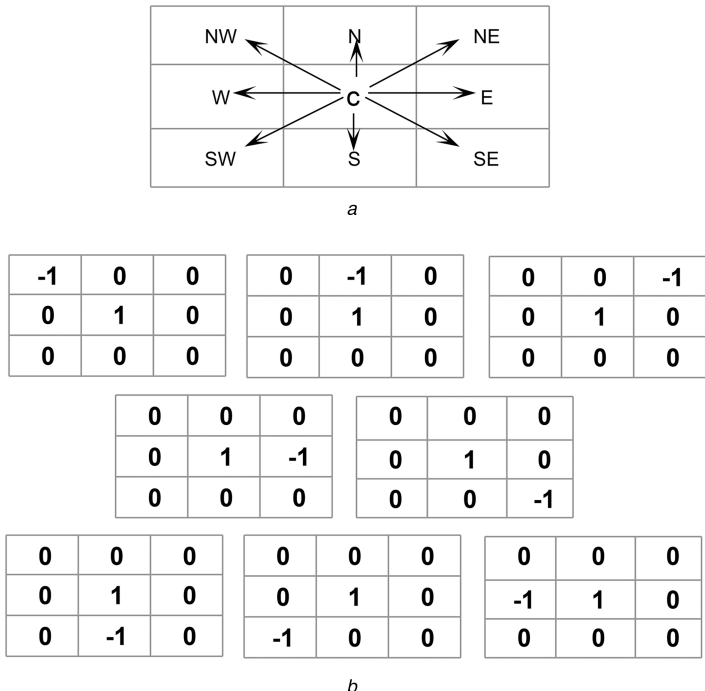


**Fig. 2** Images represent

(a) Eight  $3 \times 3$  directional neighbours of  $c$ , (b) Eight  $3 \times 3$  convolution masks

If  $\alpha(i, j) = 1$ , then  $(i, j)$ th pixel in  $I$  is possibly noisy; else it is noiseless. The possibly noisy sets are considered as noisy if they are SPN. But in some cases, images might have '0' & '255' as their original intensities and for eliminating such redundancy about possibility of the noisiness, the second noise detection has been implemented to identify appropriate noisy candidates.

### 3.2 Second noise detection unit

This section describes about the construction of FSs and their corresponding IFSs. Finally, a threshold is obtained based on entropy to determine the noisy pixels.

**3.2.1 Construction of FSs:** The shortcoming in the first detection mechanism is in finding an appropriate threshold  $T$  for the noisy image  $I$ . Numerous denoising methods exist in literature to find threshold value using FS theory. In the proposed method, several thresholds are obtained using the method in [30], among those multiple thresholds a single appropriate threshold will be chosen using minimum entropy concept. In the proposed method, the width of the FS is taken into account. By varying  $w$  new membership functions are obtained using

$$\mu_{F_{sw}}(I(i, j)) = \begin{cases} e^{-|I(i, j) - mb(s)|/w}, & \text{if } I(i, j) < s \\ e^{-|I(i, j) - mo(s)|/w}, & \text{if } I(i, j) \geq s, \end{cases} \quad (4)$$

with

$$mb(s) = \frac{\sum_{I(i, j)=0}^s I(i, j) \cdot h(I(i, j))}{\sum_{I(i, j)=0}^s h(I(i, j))} \quad \text{and}$$

$$mo(s) = \frac{\sum_{I(i, j)=s+1}^{L-1} I(i, j) \cdot h(I(i, j))}{\sum_{I(i, j)=s+1}^{L-1} h(I(i, j))}$$

representing the mean intensity of the pixels that belongs to the background and the foreground (object) respectively,  $h(I(i, j))$  counts the pixels of the image with brightness value  $I(i, j)$  and a free constant argument  $w \in [1, (L=256)]$ . Hence, one can generate  $256^2$  FSs by varying  $s$  and  $w$ . In order to reduce the computational complexity and keep the values of the membership function in the range  $[0.5, 1]$ , hence  $w$  is chosen such that the membership values lie on this defined interval. Suppose if

$w_1, w_2, \dots, w_n$  are the parameters that lie on the interval  $[1, L]$  such that the image  $I$  has its membership values in the range  $[0.5, 1]$ , then  $n$  FSs can be generated for the image  $I$ . Hence for  $n$  FSs,  $n$  thresholds are obtained by generating IFSs and its construction is described in the next section. Let  $F_{st}$  denoted the fuzzy image, which is a coupling of the fuzzy foreground  $F_{O_{st}}$  and the background  $F_{B_{st}}$  of the image  $I$ , for each  $s = \{0, 1, \dots, L-1\}$  and  $t = \{1, 2, \dots, n\}$ .

**3.2.2 Generation of IFSs:** For finding the threshold of an image, one should perfectly separate the object from the background. This accurate separation depends on the design of the membership function, where the user lacks about such design. In this paper, the intuitionistic fuzzy index ( $\pi$ ) of IFS  $A$  is regarded as the hesitation of user in constructing the degree of pixel belonging to the background or the object. Consider  $\mu_{F_{O_{st}}}$  and  $\mu_{F_{B_{st}}}$  are the  $n L$ -membership functions of the object and the background pixels in the image, respectively. For each brightness level  $s$  and  $t$ , intuitionistic fuzzy index  $\pi_{st}$  should satisfy the following criteria:

- i. The index  $\pi_{st}(I(i, j))$  depends only on  $\mu_{F_{O_{st}}}$  and  $\mu_{F_{B_{st}}}$ .
- ii. If the user is certain in segregation of the pixel  $I(i, j)$  of the noisy image either to an object or the background, then  $\pi(I(i, j)) = 0$ .

Then  $n L$ -IFSs related to the object ( $F_{O_{st}}$ ) and the background ( $F_{B_{st}}$ ) of the image  $I$  are constructed for each intensity level  $s = \{0, 1, \dots, L-1\}$  and  $t = \{1, 2, \dots, n\}$ . They are constructed in such a way that each pixel of the image  $I$  is linked with three values:

- i. A value consisting of its membership to the background/object of the image and is pertained to the knowledge of the user.
- ii. A value consisting of its non-membership to the background/object of the image and is related to the knowledge of the user.
- iii. A value consisting of the hesitation  $\pi$  of the user in deciding the membership explained in 1 and 2 above.

Hence, for each  $s = \{0, 1, \dots, L-1\}$  and  $t = \{1, 2, \dots, n\}$ ,  $\pi_{st}(g)$  is expressed as

$$\pi_{st}(I(i, j)) = (1 - \mu_{F_{B,st}}(I(i, j))) \cdot (1 - \mu_{F_{O,st}}(I(i, j))), \quad (5)$$

where the values of  $\mu_{F_{B,st}}$  and  $\mu_{F_{O,st}}$  lie on the interval  $[0.5, 1]$  from the definition of membership function in (4). That is,  $0.5 \leq \mu_{F_{B,st}}, \mu_{F_{O,st}} \leq 1$ , which implies  $0 \leq 1 - \mu_{F_{B,st}}, 1 - \mu_{F_{O,st}} \leq 0.5$ .

Using (5),  $n$   $L$ -IFSs  $A_{B,st}$  of the background are constructed corresponding to the FSs  $F_{B,st}$  as

$$A_{B,st} = \{\langle I(i, j), \mu_{F_{B,st}}(I(i, j)), \nu_{F_{B,st}}(I(i, j)), \pi_{st}(I(i, j)) \rangle\}, \quad (6)$$

where  $\nu_{F_{B,st}}(I(i, j)) = 1 - \mu_{F_{B,st}}(I(i, j)) - \pi_{st}(I(i, j)), 0 \leq I(i, j) \leq L$ .

**3.2.3 Determination of threshold based on entropy:** Entropy of an image  $A$  is calculated using

$$E(A_{st}) = \frac{1}{\text{card}(I)} \sum_{I(i,j)=0}^{L-1} h(I(i, j)) \cdot \pi_{st}(I(i, j)), \quad (7)$$

where  $\text{card}(I)$  denotes the cardinality of pixels in the image  $I$ ,  $s = \{0, 1, \dots, L-1\}$  and  $t = \{1, 2, \dots, n\}$ .

Now let us discuss the range of the entropy of these IFSs. On looking into the right-hand side terms of (7),  $\pi_{st}(I(i, j)) = (1 - \mu_{F_{B,st}}(I(i, j))) \cdot (1 - \mu_{F_{O,st}}(I(i, j))) \leq (0.5) \cdot (0.5) = 0.25$ .

Since  $h(I(i, j))$  enumerates the count of  $I(i, j)$  in the image  $I$  with cardinality  $\text{card}(I)$ ,  $\sum h(I(i, j)) \leq \text{card}(I)$ . That is, the possible maximum value of  $\sum h(I(i, j))/\text{card}(I)$  is 1. Therefore from (7), the entropy of  $A_{st}$  lies on the interval  $[0, 0.25]$ . For more details, see [31].

The entropy  $E$  for each one of  $n$   $L$ -IFSs  $A_{st}$  associated with the image  $I$  is computed. Then  $n$  IFSs with least entropy from these  $n$   $L$ -IFSs for each  $t = \{1, 2, \dots, n\}$  and opt that  $s$  as a best threshold. Therefore for a single  $s$ , one can obtain  $n$  thresholds are obtained for the image  $I$ . Pick the best threshold  $t$  by taking modal value of the  $n$  thresholds. If there is no such modal value, then threshold is obtained by taking median of these  $n$  thresholds.

### 3.3 Noise detection

One can clearly notice that the impulse noise bears similarity with the high-frequency content of images like edges and fine details because both reflect sudden changes in pixel values. So, the main aim of this study is to identify the pixels affected by impulse noise using the concept of difference of the concerned pixel value with respect to mean intensity of the pixels in the neighbourhood of specified window size. That is, a pixel with higher noise will have a larger difference with the median intensity. For more details one can refer, [32]. Since, proposed method considers two means: one related to the background and other related to the object, so the membership function for finding noisy candidate is defined as follows:

$$\alpha(i, j) = \begin{cases} 0, & \text{if } |I(i, j) - a| < a; \\ \frac{|I(i, j) - a|}{b - a}, & \text{if } a \leq |I(i, j) - (a + b)/2| < b; \\ 1, & \text{if } |I(i, j) - b| \geq b, \end{cases} \quad (8)$$

where  $a = mb(t)$  and  $b = mo(t)$  are the mean intensity of the background and the object at the threshold  $t$ .

### 3.4 Noise removal using fuzzy logic

The robustness of a set of noisy pixels can be determined by combining the set of pixels from both the detection units (from (3) and (8)). The output of the fuzzy filter is

$$O(i, j) = \alpha(i, j) \cdot m(i, j) + (1 - \alpha(i, j)) \cdot I(i, j), \quad (9)$$

where  $m$  denotes the median value of  $3 \times 3$  neighbourhood of  $(i, j)$ th pixel of the image  $I$ .

## 4 Experimental analysis

In this section, the proposed algorithm and the state-of-the-art methods AWMF [4], AFSWAF [12], NAFSMF [15], MDBUTMF [16] and IATMF [5] are used to study the performance in the presence of impulse noise. Several tests are executed on numerous eight-bit images with various levels of noise including grey scale, colour and medical images. Few of them are provided in this paper in order to show the performance of the proposed method over five other existing methods. The parameters of each existing method in the experimental study are briefly given as follows. In the method NAFSMF, the two thresholds of fuzzy membership functions extracting local information are fixed as 10 and 30 with maximum window size is  $3 \times 3$ . For the method MDBUTMF, the adaptive window size is taken as  $3 \times 3$ . In AFSWAF technique at the stages of impulse detection, finding set of uncorrupted pixel set, fuzzy similarity membership function, thresholds are set as 15, 0.5 and 4 and all window sizes during detection are chosen as  $3 \times 3$ . In AWMF method of denoising, initial window size is fixed as  $3 \times 3$  and final maximum window size is fixed as  $5 \times 5$ . For the iterative method IATMF, number of iteration is taken as 1,  $h_{\min} = 0.8$  and  $h_{\max} = 0.9999$  and the maximum filtering window size is taken as  $5 \times 5$ . The performance of the denoising techniques is evaluated using peak-signal-to-noise ratio (PSNR) and error rate (ER) along with the time for computation.

The quality of denoised image is evaluated using PSNR. PSNR can be computed using

$$\text{PSNR} = 10 \log_{10} \frac{(L-1)^2}{\text{MSE}},$$

where  $\text{MSE} = (1/MN) \sum_{i=1}^M \sum_{j=1}^N (I(i, j) - R(i, j))^2$  is the mean square error, in which  $I$  and  $R$  denote the original and denoised images with size  $M \times N$ . The PSNR will be high when the original and denoised images are similar.

Percentage of error or ER in the denoised image is defined as

$$\text{ER} = \frac{\text{Card}(C)}{MN} \times 100\%.$$

where  $C = \{(i, j) \in R : I(i, j) \neq R(i, j)\}$  and  $\text{Card}(C)$  denotes cardinality of the set  $C$ .

Boat image with 20% SPN is denoised using five existing filtering methods along with the proposed method and their corresponding results are shown in Fig. 3. Figs. 3a and h show the 20% noisy and original Boat images, respectively. Filtered results of Boat image with 20% SPN that are denoised using MDBUTMF, NAFSMF, AFSWAF, AWMF and IATMF are portrayed in Figs. 3b–g, respectively. On observing all these figures, Fig. 3g has highly clear edges without blurriness than other five existing methods. Qualitatively one can reveal that the proposed method reduces noise well than the comparable methods.

Lena image with 70% SPN is denoised by the proposed method along with the five comparative state-of-the-art methods, which are qualitatively picturised in Fig. 4. Figs. 4a and h, respectively, show the Lena image with 70% SPN and a clear original image without SPN. Filtered results of Lena image with 70% noise obtained by MDBUTMF, NAFSMF, AFSWAF, AWMF, IATMF and the proposed method are shown in Figs. 4b–g, respectively. On observing the Fig. 4b, it is clear that the method MDBUTMF leaves some noisy pixels undetected and retained in the image as hazy pixel. Some noisy dot remains randomly spread out in Fig. 4c, which is acquired by utilising NAFSMF. Edges of Figs. 4d–f look fuzzy and fine details are unclear while comparing with that of Fig. 4h. But from Fig. 4g qualitatively one can be assured that the proposed algorithm denoised the noisy pixels perfectly.

The PSNR values of 15 various grey scale images including medical images with various levels of SPN, denoised by different methods are shown in Table 1. The PSNR values of NAFSMF,

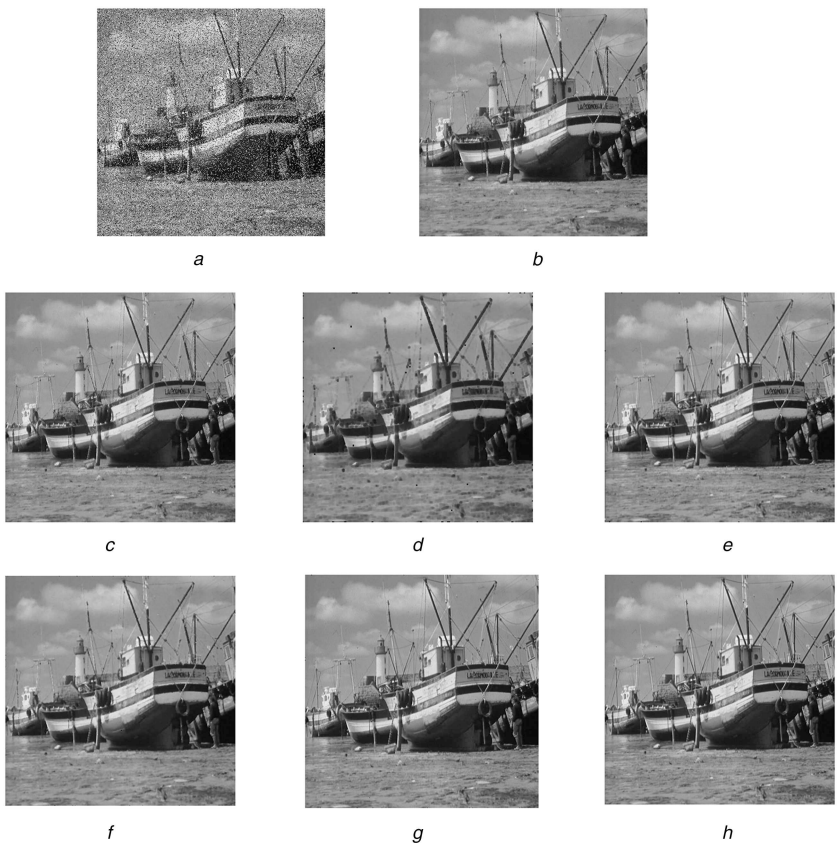


**Fig. 3** Denoised results of boat image using various filters

(a) 20% Noisy image, (b) MDBUTMF, (c) NAFSMF, (d) AFSWAF, (e) AWMF, (f) IATMF, (g) Proposed method, (h) Original boat image

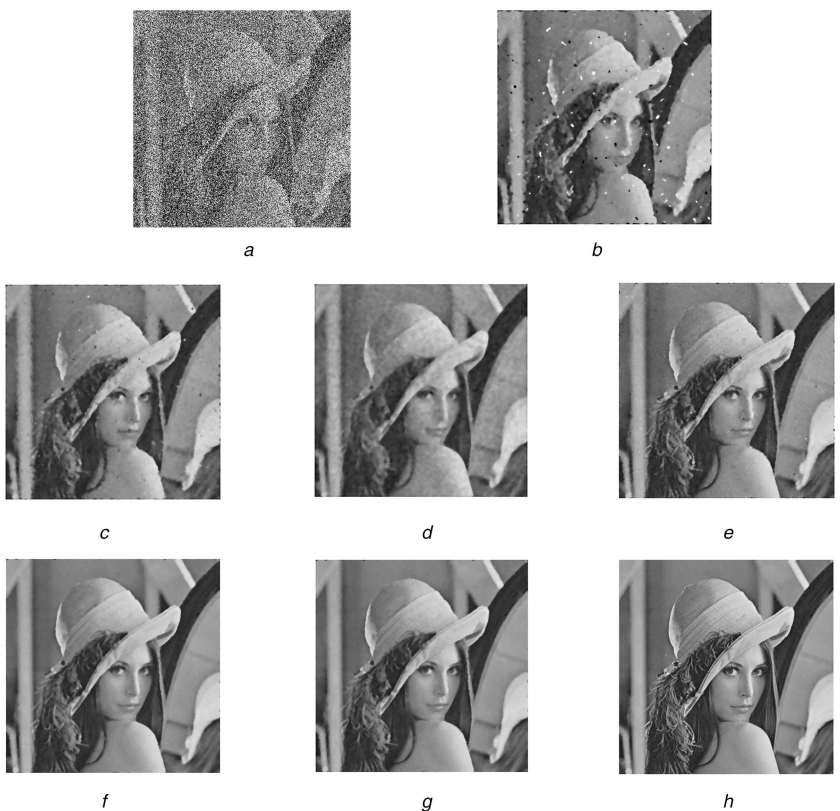


**Fig. 4** Denoised results of Lena image by various filters

(a) 70% Noisy image, (b) MDBUTMF, (c) NAFSMF, (d) AFSWAF, (e) AWMF, (f) IATMF, (g) Proposed method, (h) Original Lena image

MDBUTMF, AFSWAF, AWMF and IATMF are lower when compared with the proposed method. If the PSNR is higher, then the similarity between original and denoising images is higher. Table 1 demonstrates that the proposed method works better than

comparative methods quantitatively for all the images with various levels of SPN.

Denoised results of MRI brain and Lymphocyte images affected with 40 and 60% SPN are portrayed in Figs. 5 and 6, respectively

**Table 1** PSNR value of the 15 denoised images using different filters

Image	Noise per cent, %	MDBUTMF	NAFSMF	AWSWF	AWMF	IATMF	Proposed algorithm
Boat	20	31.3151	31.8892	29.0506	32.2653	36.0312	<b>37.0353</b>
	50	27.5086	27.4429	26.9710	30.1236	30.6892	<b>32.0220</b>
	80	24.9142	24.2109	25.1157	28.0927	28.1801	<b>29.3828</b>
Bridge	20	27.6889	28.2085	27.1242	30.4700	31.6820	<b>33.4916</b>
	50	24.2174	24.1841	26.1434	27.1265	27.4371	<b>30.6084</b>
	80	21.3988	21.1247	24.0925	24.2500	24.3145	<b>28.5084</b>
Cameraman	20	28.4725	28.8728	33.2511	34.2310	34.4181	<b>36.6202</b>
	50	24.7989	24.6868	30.7723	30.7042	30.1252	<b>32.2487</b>
	80	21.5660	21.7682	28.5937	28.7494	28.7024	<b>29.7337</b>
Coco	20	36.2263	37.9860	31.6889	36.0451	38.0746	<b>40.0178</b>
	50	33.0087	33.0116	27.9255	30.1226	30.6036	<b>31.8380</b>
	80	28.6409	28.5004	25.2626	27.1960	27.5630	<b>28.9350</b>
Flinstones	20	26.0828	26.3238	27.8429	30.9758	32.8883	<b>34.4673</b>
	50	22.0191	22.0210	24.5259	29.5826	27.1093	<b>31.0216</b>
	80	18.8059	18.7773	18.2068	24.9366	21.3992	<b>28.7890</b>
Goldhill	20	33.2991	33.9447	29.1436	32.4259	34.6369	<b>36.7771</b>
	50	29.7416	29.6303	26.9883	27.2879	30.5367	<b>31.3924</b>
	80	26.6072	26.3257	22.0679	24.1824	26.4267	<b>28.7596</b>
House	20	34.1309	34.9962	34.4430	36.5982	38.9820	<b>40.0502</b>
	50	30.5439	30.2119	30.6374	32.9350	33.2916	<b>34.9961</b>
	80	26.5150	26.0811	28.0114	28.9545	28.2481	<b>29.9546</b>
Mandrill	20	27.4799	27.5905	27.4106	30.0032	31.0708	<b>33.3113</b>
	50	23.4366	23.4223	26.1800	29.1606	29.4413	<b>30.4636</b>
	80	20.7639	20.7507	24.9372	26.8627	27.0490	<b>28.4607</b>
Lena	20	34.5112	35.7006	39.6252	36.8065	37.5763	<b>40.9555</b>
	50	31.0303	31.1129	33.8830	32.1703	30.5268	<b>34.8305</b>
	80	27.4509	26.9439	28.1449	28.9917	28.1588	<b>29.4625</b>
Peppers	20	25.0848	25.2434	29.3608	31.4479	37.9911	<b>39.7019</b>
	50	23.9884	23.9923	27.1439	29.5839	32.3424	<b>33.4440</b>
	80	22.1176	21.8936	25.2049	27.9331	27.5134	<b>28.9404</b>
Breast	20	44.5195	41.7502	18.4222	33.2329	48.7962	<b>48.9971</b>
	50	34.6764	37.5773	13.3672	16.1435	38.6188	<b>45.8853</b>
	80	17.9088	32.5634	10.4140	8.0363	34.6255	<b>38.5003</b>
Kidney	20	40.4223	42.4213	17.3890	34.1155	39.9260	<b>49.6113</b>
	50	33.0418	35.0137	13.1412	16.9455	38.9305	<b>42.9141</b>
	80	20.2410	30.1931	10.7772	8.7468	36.6168	<b>43.8823</b>
Liver	20	21.6110	22.2414	14.5814	18.7320	39.8849	<b>41.5676</b>
	50	20.8465	21.2789	11.8487	13.4492	29.9354	<b>30.7771</b>
	80	15.8459	19.4672	9.6372	7.6986	20.8728	<b>21.4189</b>
Lymphocytes	20	42.4052	38.8993	16.0072	31.4645	44.8787	<b>48.9221</b>
	50	32.6135	33.6694	11.6891	15.5822	39.1034	<b>40.0354</b>
	80	17.2217	28.5782	9.0123	7.7539	30.6499	<b>42.0012</b>
MRI brain	20	22.2132	23.0630	14.2030	16.8295	25.2500	<b>32.8328</b>
	50%	15.9891	15.4528	9.8512	12.1854	20.9100	<b>29.5934</b>
	80	11.2687	11.3731	7.2528	6.4612	18.8309	<b>25.6238</b>

to show the effectiveness of proposed method on medical images. Images obtained by using the proposed denoising method seem to detect noisy candidates considerable more when compared with other existing methods. A major reason for such improved result made by the proposed method is that it opts noisy candidate without regarding extreme intensity values.

Mean PSNR values of denoised results of Lena image with 70% SPN, MRI brain image with 40% SPN and Lymphocyte image with 60% SPN are given in Table 2. Since PSNR rate of the proposed method seems to be high, which concludes that the proposed method is more effective for detection and smoothing the noisy pixels in images than the other five existing methods.

In the denoised image, ER is computed for 15 images under different noise levels and their average values are shown in Fig. 7. From Fig. 7, AWMF and IATMF have less ER than other comparative methods such as MDBUTMF, NAFSMF and AWSWF. Since the ERs of the other five existing methods are

high when compared with the proposed method, IFS-based denoising method detects noisy pixels appropriately.

Computation time for various filtering methods is calculated in seconds for 15 images. Average processing times for those 15 images at different levels of noise by various filtering methods are shown in Fig. 8. The proposed method has relatively less processing time with respect to comparative filtering methods. Computation time is high for other methods; this may be due to some reasons which are described below. Time computation for denoising the SPN-affected images by using AWSWF are higher than all other existing methods, since it searches noisy candidates by finding uncorrupted ones by a series of process in determination and validation of such selection with various thresholds several times. IATMF seems to have the next largest time for computation during denoising. This is due to the reason that it evaluates good pixel set with certain criteria defined in each window of size  $5 \times 5$  and this size may increase, if necessary, throughout the whole

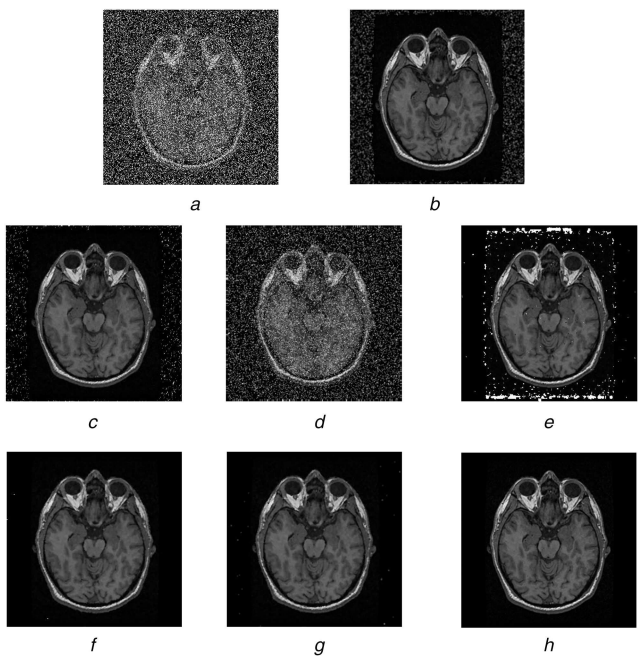


**Fig. 5** Denoised results of MRI brain image by various filters  
(*a*) 40% Noisy image, (*b*) MDBUTMF, (*c*) NAFSMF, (*d*) AFSWAF, (*e*) AWMF, (*f*) IATMF, (*g*) Proposed method, (*h*) Original MRI brain image

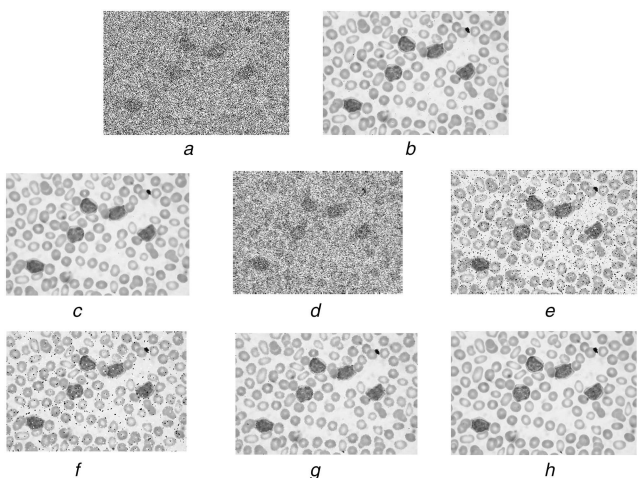


**Fig. 6** Denoised results of Lymphocyte image by various filters  
(*a*) 60% Noisy image, (*b*) MDBUTMF, (*c*) NAFSMF, (*d*) AFSWAF, (*e*) AWMF, (*f*) IATMF, (*g*) Proposed method, (*h*) Original Lymphocyte image

image during processing. MDBUTMF requires less time for processing when compared with AFSWAF and IATMF. In AWMF, maximum window size is fixed as  $5 \times 5$ , median of such matrix needs less time when compares to AFSWAF. NAFSMF needs lower computational time than AFSWAF, but is higher than the time consumed by the proposed method. Since adaptive filter window size of NAFSMF method is fixed as  $3 \times 3$  and two thresholds are assumed as 10 and 30, while detection makes computation time lower. Then, median of that fixed window is chosen as the filtered output of NAFSMF. Hence, NAFSMF needs less time than that the time required for searching some termination criteria defined in IATMF and AFSWAF. But the proposed method finds the threshold value for separating the noisy candidates and it does not utilise some radius of neighbour pixels and its behaviour during such computation. Hence, the proposed method needs much

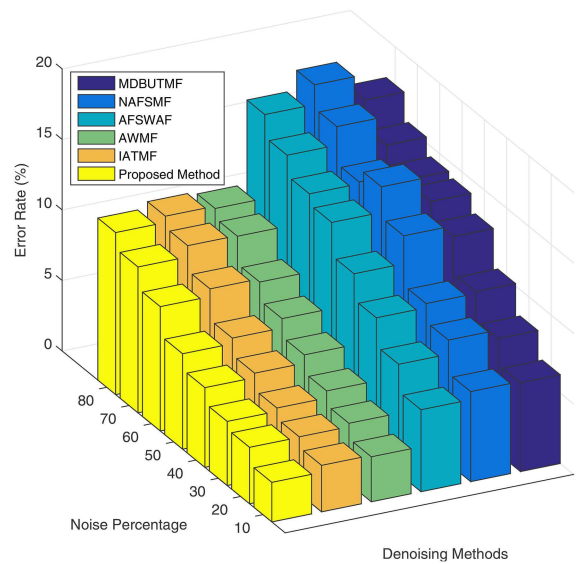


**Fig. 7** Mean ERs of denoised 15 images by various denoising techniques

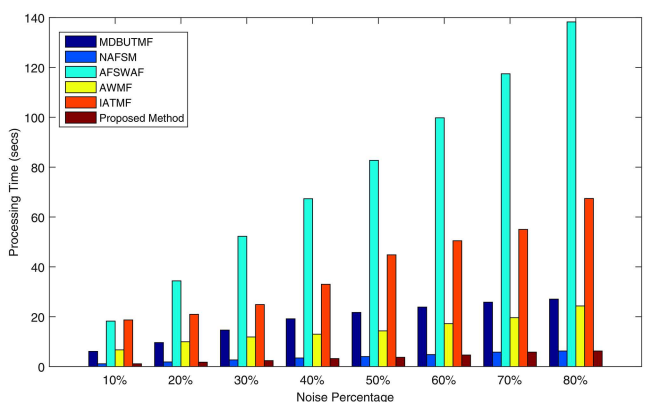


**Fig. 8** Average computational time (15 grey images) of the proposed filter and comparative methods at different degrees of noise levels

less time when compared to other five existing methods. Similarly, 80% SPN affected Mandrill image and its original image are portrayed in Figs. 9*a* and *h*. Fig. 9*a* is denoised using MDBUTMF, NAFSMF, AFSWAF, AWMF, IATMF, along with the proposed method and their results are respectively, given in Figs. 9*b*–*g*. MDBUTMF produced better result in denoising colour image than that of the grey scale images. Also, other four existing techniques generate less denoising effect since they search the intensities in a large window size. Application of such erroneous search in each channel of colour Mandrill image has produced more dots in the results acquired using the four existing denoising techniques such as NAFSMF, AFSWAF, AWMF and IATMF. But the proposed method does not search such values, so it makes perfect suggestion for denoising the correct noisy candidate. These make the proposed method to produce good result than other five existing methods.

To evaluate the performance of denoising techniques for the removal of SPN in colour images, PSNR rates for each Red channel (R-channel), Green channel (G-channel) and Blue channel (B-channel) of colour images are separately analysed. Average PSNR rates of each channel of Mandrill images are portrayed in the Table 3. In Table 3, MDBUTMF has high PSNR rate for G and B channels than the corresponding channels of other four existing methods. NAFSMF has next highest PSNR rate when compared with AFSWAF, AWMF and IATMF for all the three channels. Also, it is clearly that AFSWAF produces less PSNR value than

**Table 2** Mean PSNR value of the denoised MRI brain, lymphocyte and Lena images with 40, 60 and 70% SPN acquired using several filters

	MDBUTMF	NAFSMF	AFSWAF	AWMF	IATMF	Proposed algorithm
PSNR	27.6334	28.5072	29.8482	31.0723	28.8813	<b>31.5692</b>

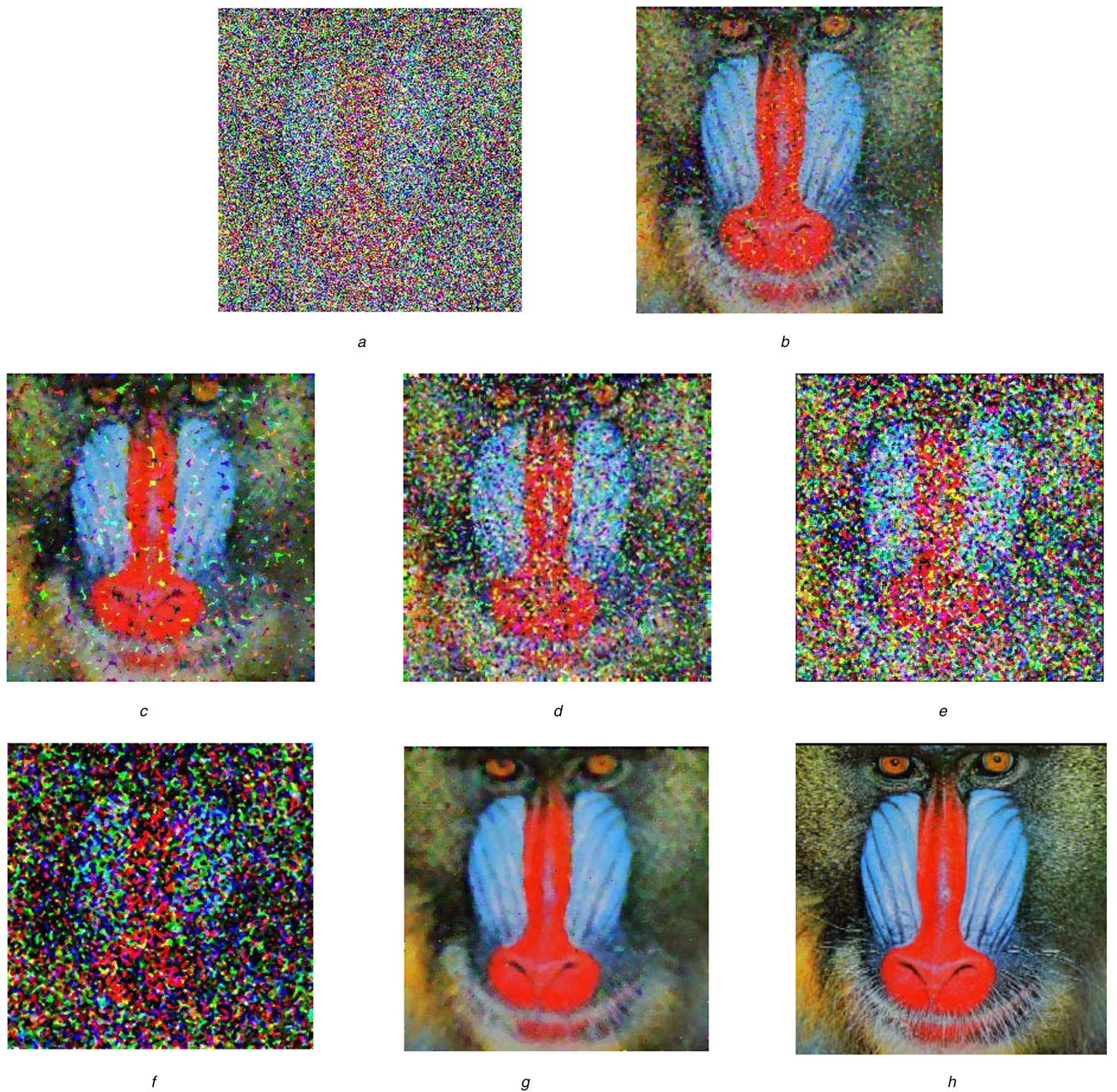


**Fig. 9** Denoised results of Mandrill image by various filters

(a) 80% Noisy image, (b) MDBUTMF, (c) NAFSMF, (d) AFSWAF, (e) AWMF, (f) IATMF, (g) Proposed method, (h) Original Mandrill image

**Table 3** PSNR value of the denoised Mandrill colour images with 80% SPN acquired using several filters

Colour	MDBUTMF	NAFSMF	AFSWAF	AWMF	IATMF	Proposed algorithm
red	11.6556	14.7749	11.1310	12.8545	12.4093	<b>16.8243</b>
green	16.0852	14.9654	11.2642	13.1092	12.5763	<b>17.5810</b>
blue	15.1977	14.6145	11.0009	12.6259	12.0394	<b>16.9982</b>

other comparable methods. But among all the four methods, MDBUTMF showed better performance, which is comparatively lower than the rates of the proposed method. Hence, the proposed method renders better denoised results than other comparable methods. Time computation for denoising colour image by each method is equal to thrice the time required to denoise a single grey scale image by the corresponding methods. Similarly, ER values are also trice the ER values generated for single grey scale image. The proposed method eliminated noise without degrading the fine lines and edges. Therefore, the proposed method is better in removing noise without distortion of image features than comparative methods. Also when the level of noise is high, the

IFS-based denoising method is more efficient in reducing noise than comparative techniques both visually and quantitatively.

## 5 Conclusion

This paper introduces the application of IFS for impulse noise reduction in the images. Since hesitation degree in IFS plays a vital role in removing vagueness, IFS has been implemented to remove vagueness in assigning membership values to the image pixels. Also, the proposed method denoised the image without considering their extreme values. The proposed method and the existing methods have been experimentally analysed with images of different per cent of impulse noise. Denoised images portray that

the proposed method have reduced noise well than the five existing methods. Primary argument about the betterment of the proposed method is that IFS absorbs much more uncertainty than FS. In future, perhaps the iterative technique can be incorporated to this method in interval-valued intuitionistic fuzzy domain to deal with other type of noises.

## 6 Acknowledgments

This work was supported by the UGC-BSR (Research fellowship in Mathematical Sciences-2013-2014), Government of India, New Delhi. It is also supported by the Engineering Faculty of the University of Malaya under Grant No. UM.C/625/1/HIR/MOHE/ENG/42. The authors would like to thank all reviewers and editors for their fruitful comments and suggestions for significant improvement of the manuscript.

## 7 References

- [1] Teuber, T., Remmeli, S., Hesser, J., et al.: 'Denoising by second order statistics', *Signal Process.*, 2012, **92**, (12), pp. 2837–2847
- [2] Bhadouria, V.S., Ghoshal, D.: 'A study on genetic expression programming-based approach for impulse noise reduction in images', *Signal Image Video Process.*, 2016, **10**, (3), pp. 575–584
- [3] Wu, J., Tang, C.: 'Random-valued impulse noise removal using fuzzy weighted non-local means', *Signal Image Video Process.*, 2015, **8**, (2), pp. 349–355
- [4] Zhang, P., Li, F.: 'A new adaptive weighted mean filter for removing salt-and-pepper noise', *IEEE Signal Process. Lett.*, 2014, **21**, (10), pp. 1280–1283
- [5] Ahmed, F., Das, S.: 'Removal of high-density salt-and-pepper noise in images with an iterative adaptive fuzzy filter using alpha-trimmed mean', *IEEE Trans. Fuzzy Syst.*, 2014, **22**, (5), pp. 1352–1358
- [6] Kayhan, S.K.: 'An effective 2-stage method for removing impulse noise in images', *J. Vis. Commun. Image R.*, 2014, **25**, (2), pp. 478–486
- [7] Yang, R., Yin, L., Gabouj, M., et al.: 'Optimal weighted median filtering under structural constraints', *IEEE Trans. Signal Process.*, 1995, **43**, (3), pp. 591–604
- [8] Lin, H.M., Willson, A.N.Jr.: 'Median filters with adaptive length', *IEEE Trans. Circuits Syst.*, 1988, **35**, pp. 675–690
- [9] Chen, T., Ma, K.K., Chen, L.H.: 'Tri-state median filter for image denoising', *IEEE Trans. Image Process.*, 1999, **8**, pp. 1834–1838
- [10] Zhang, S., Karim, M.A.: 'A new impulse detector for switching median filters', *IEEE Signal Process. Lett.*, 2002, **9**, (11), pp. 360–363
- [11] Chen, T., Hong, R.W.: 'Adaptive impulse detection using center-weighted median filters', *IEEE Signal Process. Lett.*, 2001, **8**, (1), pp. 1–3
- [12] Varghese, J., Ghouse, M., Subash, S., et al.: 'Efficient adaptive fuzzy-based switching weighted average filter for the restoration of impulse corrupted digital images', *IET Image Process.*, 2014, **8**, (4), pp. 199–206
- [13] Wang, Z., Zhang, D.: 'Progressive switching median filter for the removal of impulse noise from highly corrupted images', *IEEE Trans. Circuits Syst. II, Analog Digit. Signal Process.*, 1999, **46**, pp. 78–80
- [14] Ng, P., Ma, K.: 'A switching median filter with boundary discriminative noise for extremely corrupted images', *IEEE Trans. Image Process.*, 2006, **15**, (6), pp. 1506–1516
- [15] Toh, K.K.V., Isa, N.A.M.: 'Noise adaptive fuzzy switching median filter for salt-and-pepper noise reduction', *IEEE Signal Process. Lett.*, 2010, **17**, (3), pp. 281–284
- [16] Esakkirajan, S., Veerakumar, T., Subramanyam, A.N., et al.: 'Removal of high density salt and pepper noise through modified decision based unsymmetric trimmed median filter', *IEEE Signal Process. Lett.*, 2011, **18**, (5), pp. 287–290
- [17] Lu, L., Jin, W., Wang, X.: 'Non-local means image denoising with a soft threshold', *IEEE Signal Process. Lett.*, 2014, **22**, (7), pp. 833–837
- [18] Lia, X., Hea, H., Wangb, R., et al.: 'Superpixel-guided nonlocal means for image denoising and super-resolution', *Signal Process.*, 2016, **124**, pp. 173–183
- [19] He, N., Wang, J.B., Zhang, L.L., et al.: 'An improved fractional-order differentiation model for image denoising', *Signal Process.*, 2015, **112**, pp. 180–188
- [20] Yan, R., Shao, L., Liu, L., et al.: 'Natural image denoising using evolved local adaptive filters', *Signal Process.*, 2014, **103**, pp. 36–44
- [21] Zuo, Z., Hu, J., Lan, X., et al.: 'Content-based adaptive image denoising using spatial information', *Optik-Int. J. Light Electron Opt.*, 2014, **125**, (18), pp. 5093–5101
- [22] Jain, P., Tyagi, V.: 'LAPB: Locally adaptive patch-based wavelet domain edge-preserving image denoising', *Inf. Sci.*, 2015, **294**, (10), pp. 164–181
- [23] Pham, C.C., Jeon, J.W.: 'Efficient image sharpening and denoising using adaptive guided image filtering', *IET Image Process.*, 2015, **9**, (1), pp. 71–79
- [24] Sulaiman, S.N., Isa, N.A.M., Yusoff, I.A., et al.: 'Switching-based clustering algorithms for segmentation of low-level salt-and-pepper noise corrupted images', *Signal Image Video Process.*, 2015, **9**, (2), pp. 387–398
- [25] Xu, L., Li, J., Shu, Y., et al.: 'SAR image denoising via clustering-based principal component analysis', *IEEE Trans. Geosci. Remote Sens. J.*, 2014, **52**, (11), pp. 6858–6869
- [26] Zadeh, L.A.: 'Fuzzy sets', *Inf. Control*, 1965, **8**, pp. 338–353
- [27] Atanassov, K.T.: 'Intuitionistic fuzzy sets', *Fuzzy Sets Syst.*, 1986, **20**, (1), pp. 87–96
- [28] Pilevar, A.H., Saeni, S., Khandel, M., et al.: 'A new filter to remove salt and pepper noise in color images', *Signal Image Video Process.*, 2015, **9**, (4), pp. 779–786
- [29] Otsu, N.: 'A threshold selection method from gray-level histograms', *IEEE Trans. Syst. Man Cybern.*, 1979, **9**, (1), pp. 62–66
- [30] Ananthi, V.P., Balasubramaniam, P., Lim, C.P.: 'Segmentation of gray scale image based on intuitionistic fuzzy sets constructed from several membership functions', *Pattern Recognit.*, 2014, **47**, pp. 3870–3880
- [31] Melo-Pinto, P., Couto, P., Bustince, H., et al.: 'Image segmentation using Atanassov's intuitionistic fuzzy sets', *Expert Syst. Appl.*, 2013, **40**, (1), pp. 15–26
- [32] Azimirad, E., Haddadnia, J.: 'Design of a new filtering for the noise removing in images by fuzzy logic', *J. Intel. Fuzzy Syst.*, 2015, **28**, (4), pp. 1869–1876